J. Fluid Mech. (1971), *vol.* 45, *part* 2, *pp.* 321–339
Printed in Great Britain

Two problems in the gravity flow of granular materials

By M. A. GOODMAN† AND S. C. COWIN
Department of Mechanical Engineering, Tulane University, New Orleans, La.

(Received 2 January 1970 and in revised form 27 July 1970)

Two problems representative of the gravity flow of granular materials are considered in the context of a theory presented by Goodman (1970). The problems consist of steady fully-developed flow of a granular material down an inclined plane and between vertical parallel plates. It is shown that the dynamical behaviour of these materials is quite different from that of a viscous fluid. For the inclined flow problem, the normal stresses are not only unequal but vary non-linearly with depth. Also the maximum value of the mass flux distribution does not necessarily occur at the upper surface. For the vertical channel-flow problem, the material behaves somewhat like a Bingham fluid in that a plug region exists in the central part of the channel. The interesting feature of this problem is that the concentration of material volume in the shearing region outside the plug may either increase or decrease from the plug to the channel wall, depending on the boundary conditions. Experimental evidence for these phenomena in real granular materials is cited.

The results of this investigation suggest that the gravity flow of granular materials is essentially governed by two factors—a material characteristic length, which is possibly related to the grain size, and the externally imposed constraints such as the gravity field or the pressure exerted upon the granular material from the confining plates.

1. Introduction

An analytical model for the dynamical behaviour of granular materials is essential to the solution of a wide range of problems associated with the handling and movement of materials such as soils, sands, grains, fibres, and powders. There are two approaches to the modelling of granular materials, the particulate approach and the continuum approach. In the particulate approach one considers an ensemble of particles of finite size (idealized, say, as rigid or elastic spheres) and attempts to deduce the laws governing the mechanical behaviour of the entire ensemble. Notable qualitative insight into the mechanical behaviour of cohesionless granular materials has been obtained with this approach by Reynolds (1885), Deresiewicz (1958), Rowe (1962), and Winterkorn (1966). The continuum approach, on the other hand, assumes that the material properties of the ensemble may be represented by continuous functions so that the medium may be divided indefinitely without losing any of its defining properties. In this case, the notion

† Present address: Esso Production Research Co., Houston, Texas.

of discrete granules is no longer retained. Continuum plasticity type models based on the Mohr–Coulomb criterion for failure have been proposed by Drucker & Prager (1952), Shield (1955), Drucker, Gibson, & Henkel (1957), Jenike & Shield (1959), and Spencer (1964). In the area of fluidization, continuum models for granular materials have been investigated by Leva (1959), Zenz & Othmer (1960), and Soo (1967). A mathematical theory for fluidized beds incorporating the idea of granule distribution has been formulated by Murray (1965). A basic premise underlying the present investigation is that a continuum model can be employed for characterizing the dynamical behaviour of granular materials.

In § 2 the concept of volume distribution in a granular material is introduced and discussed. In §§ 3 and 4 an appropriate dynamical representation for the stress is developed, and in § 5 the equations governing the flow of granular materials are recorded. An inclined gravity-flow problem is considered in § 6 and a vertical channel-flow problem is considered in § 7. The results of this study and the related experimental work are discussed in § 8.

2. The volume distribution function

The distribution of the solid granular constituent in granular materials is a distinguishing characteristic of these materials. To account for the distribution of solid volume in a granular body, a kinematical variable ν, called the *volume distribution* function, is introduced as a continuous function defined over the body. The volume distribution function serves as a continuum analogue to the concept of void ratio (actually, it is the reciprocal of one plus the void ratio). The volume distribution could also be defined as one minus the porosity. The volume $\mathscr{V}$ of granules in a granular body B is given by the integral

$$\mathscr{V} = \int_B \nu dV. \tag{2.1}$$

In a similar manner, the mass density γ of the granules themselves is introduced such that the mass $\mathscr{M}$ of granules can be expressed as

$$\mathscr{M} = \int_B \gamma\nu dV, \tag{2.2}$$

where the function $\rho(=\gamma\nu)$ is interpreted as the *bulk density* of the medium. As the mass associated with the void space is neglected, the granular mass $\mathscr{M}$ may be regarded as the total mass of the granular material. It then follows from (2.2) that the continuity equation for the material has the form

$$\dot{\gamma\nu} + \gamma\nu\nabla.\mathbf{v} = 0, \tag{2.3}$$

where the superimposed dot denotes the material time derivative and $\mathbf{v}$ is the spatial velocity vector. For the particular case when the granules are incompressible, i.e. $\dot{\gamma} = 0$, the expression (2.3) becomes

$$\dot{\nu} + \nu\nabla.\mathbf{v} = 0. \tag{2.4}$$

This equation is simply a conservation principle for the volume of granules and, hence, may be determined directly from (2.1). Note that although the volume of

granules remains constant, the total volume may change as evidenced by the fact that $\nabla.\mathbf{v}$ need not be zero. This idea is consistent with the concept of dilatancy in real granular materials.

Since the total mass of a granular material is given by (2.2), the conservation of linear momentum may be written as

$$\nabla.\mathbf{T}+\gamma\nu\mathbf{b}=\gamma\nu\dot{\mathbf{v}}; \quad T_{ij,j}+\gamma\nu b_i=\gamma\nu\dot{v}_i, \tag{2.5}$$

where $\mathbf{T}$ is the stress tensor and $\mathbf{b}$ is the body force vector.

3. Stress representation

A dynamical representation for the stress in granular materials was formulated by Goodman (1970). The essential results of that analysis are recorded here.

We consider first the stress representation in the equilibrium situation. It is assumed that the specific free energy ψ of the granular material depends upon the volume distribution ν and its gradient as well as upon the density γ of the granules and the temperature. Straightforward thermodynamic arguments lead to the introduction of two distinct pressures p and $\hat{p}$ and a stress vector $\mathbf{h}$ defined by

$$p=\gamma^2\nu\,\partial\psi/\partial\gamma, \quad \hat{p}=\gamma\nu^2\,\partial\psi/\partial\nu, \quad \mathbf{h}=\gamma\nu\,\partial\psi/\partial\nabla\nu. \tag{3.1}$$

Thermodynamic arguments show p, $\hat{p}$ and $\mathbf{h}$ to be related by the fundamental equation

$$\hat{p}-p=\nu\nabla.\mathbf{h}. \tag{3.2}$$

The pressure p is interpreted as a material pressure related to the compressibility of granules, whereas the pressure $\hat{p}$ is interpreted as a configuration pressure related to the volume distribution of granules. The vector $\mathbf{h}$ is called the *equilibrated stress* vector since it is associated with a system of self-equilibrating forces resulting in either a centre of compression or a centre of dilatation (cf. Love 1926, § 132). These dynamical quantities characterize the equilibrium or non-dissipative part of the stress $\mathbf{T}^0$,

$$\mathbf{T}^0=-p\mathbf{1}-\mathbf{h}\otimes\nabla\nu, \tag{3.3}$$

which, by (3.2), has the alternate representation

$$\mathbf{T}^0=-\hat{p}\mathbf{1}+\nu(\nabla.\mathbf{h})\,\mathbf{1}-\mathbf{h}\otimes\nabla\nu. \tag{3.4}$$

From (3.3) and (3.1) it is noted that the equilibrium stress is totally derivable from the free energy function. This is analogous to the equilibrium stress in compressible fluids which is also deduced from the specific free energy function.†

The dissipative part of the stress in the theory for granular materials is similar to that of a viscous fluid,

$$\mathbf{T}-\mathbf{T}^0=\lambda(\operatorname{tr}\mathbf{D})\,\mathbf{1}+2\mu\mathbf{D}, \tag{3.5}$$

where $\mathbf{D}$ is the rate of deformation tensor defined as the symmetric part of the spatial gradient of velocity. The viscosity coefficients λ and μ are, in general, functions of γ and ν.

† The theory considered here represents a special case of a general theory which includes an *equilibrated body force* as well as an equilibrated stress $\mathbf{h}$. In the present development we have neglected the equilibrated body force.

4. Coulomb granular materials

The equilibrium stress representations (3.3) and (3.4) are too general to be amenable to problem solution. Explicit expressions for the pressures p and $\hat{p}$ and the equilibrated stress vector $\mathbf{h}$ must be obtained. To this end the specific free energy per unit volume $\gamma\nu\psi$ is assumed to be an isotropic function which is expandable in a Taylor series about $\nabla\nu = 0$ and $\nu = \nu_c$, where ν_c is the critical volume distribution corresponding to the critical void ratio.† Moreover, variations in $|\nabla\nu|$ about zero and variations in ν about ν_c are assumed to be small. From these assumptions it follows as a second-order approximation that $\gamma\nu\psi$ can be written as

$$\gamma\nu\psi = a_0 + a_1(\nu - \nu_c) + a_2(\nu - \nu_c)^2 + a_3 \nabla\nu . \nabla\nu, \tag{4.1}$$

where the coefficients are dependent on ν_c and are, at most, functions of γ. Requiring the free energy per unit volume to be positive with a minimum at $\nu = \nu_c$ and $\nabla\nu = 0$ implies that the coefficients of (4.1) are restricted by

$$a_0 \geqslant 0, \quad a_1 = 0, \quad a_2 \geqslant 0, \quad a_3 \geqslant 0. \tag{4.2}$$

Employing the representation (4.1) in (3.1) and introducing the notation

$$\alpha_0 = a_0 + a_2(\nu - \nu_c)^2, \quad \alpha = a_3, \quad \beta_0 = a_0 + a_2\nu_c^2, \quad \beta = a_2, \tag{4.3a–d}$$

yields the following expressions for p, $\hat{p}$ and $\mathbf{h}$

$$p = (\gamma\, \partial\alpha_0/\partial\gamma - \alpha_0) + (\gamma\, \partial\alpha/\partial\gamma - \alpha)\, \nabla\nu . \nabla\nu, \tag{4.4}$$

$$\hat{p} = -\beta_0 + \beta\nu^2 - \alpha \nabla\nu . \nabla\nu, \tag{4.5}$$

$$\mathbf{h} = 2\alpha\nabla\nu. \tag{4.6}$$

The equilibrium stress state (3.3) together with the representations (4.4) and (4.6) require that the equilibrium normal stress and equilibrium shear stress acting on a particular plane at a particular point bear a special relationship to one another. A similar result occurs in fluid equilibrium in that the shear stress must always vanish. In granular material equilibrium the shear stress has a specific non-zero value related to the magnitude of the normal stress. To develop this relationship consider an arbitrary but fixed point and an arbitrary but fixed plane with normal $\mathbf{n}$. Using (3.3) and (4.6) the normal stress T acting across the plane is given by

$$T = \mathbf{n} . (\mathbf{T}^0\mathbf{n}) = -p - 2\alpha(\nabla\nu . \mathbf{n})^2 \tag{4.7}$$

and is related to the shear stress S in the plane by

$$T^2 + S^2 = (\mathbf{T}^0\mathbf{n}) . (\mathbf{T}^0\mathbf{n}) = p^2 + 4\alpha p(\nabla\nu . \mathbf{n})^2 + 4\alpha^2(\nabla\nu . \nabla\nu)(\nabla\nu . \mathbf{n})^2. \tag{4.8}$$

Using (4.7) to eliminate the term $(\nabla\nu . \mathbf{n})^2$ in (4.8), completing the square in the resulting expression, and introducing the notation

$$s = \alpha\nabla\nu . \nabla\nu, \quad t = -p - \alpha\nabla\nu . \nabla\nu, \tag{4.9a,b}$$

† The critical void ratio of a granular material is the void ratio at which no volume change occurs during shearing. A granular material with a void ratio higher than the critical value decreases in volume during shear while a granular material with a void ratio lower than the critical value increases in volume during shearing.

then the relationship
$$S^2+(T-t)^2=s^2 \tag{4.10}$$

follows. Moreover, recalling the representation (4.4) for the pressure p, the expression (4.9b) can be written in the form

$$s=b(-t+c), \tag{4.11}$$

where
$$c=\alpha_0-\gamma\,\partial\alpha_0/\partial\gamma, \quad 1/b=(\gamma/\alpha)\,\partial\alpha/\partial\gamma. \tag{4.12a,b}$$

Combining (4.10) with (4.11) one obtains the sought after relationship between the shear stress S and the normal stress T acting on a particular plane at a particular point in a granular material in equilibrium. Considering S and T as Cartesian co-ordinates, (4.10) is the equation for a circle centred at $S=0$, $T=t$ with radius s. The relationship (4.11) requires that the circle radius be a function of displacement of the circle from the origin. If the relationship (4.11) is taken to be a sufficient as well as necessary condition for equilibrium, then this result is a generalization of the Coulomb stress condition of limiting equilibrium in granular materials in which the angle of internal friction and the cohesion are functions of the density γ and volume distribution ν. If b and c are constants, the traditional Mohr–Coulomb condition is obtained, i.e. the Mohr circle (4.10) is tangent to the straight line (4.11). In this case the scalar functions α_0, α, β_0, and β can be determined directly from (4.3) and the differential equations (4.12). In particular, if β_0 is taken to be a constant, then it follows from (4.12a), (4.3a), and (4.3c) that

$$\beta_0=c, \tag{4.13}$$

indicating that β_0 corresponds to the material cohesion which is positive by (4.2) and (4.3).

When (4.5) and (4.6) are combined with (3.4) and (3.5) and the Coulomb condition is used to represent the equilibrium stress, the general constitutive equation has the form

$$\left.\begin{aligned} \mathbf{T}&=(\beta_0-\beta\nu^2+\alpha\nabla\nu\,.\,\nabla\nu+2\nu\nabla\,.\,\alpha\nabla\nu)\,\mathbf{1}-2\alpha\nabla\nu\otimes\nabla\nu \\ &\qquad +\lambda(\operatorname{tr}\mathbf{D})\,\mathbf{1}+2\mu\mathbf{D} \quad \text{if} \quad \mathbf{D}\neq 0, \\ s&=b(-t+c) \qquad\qquad\qquad\qquad\qquad\quad \text{if} \quad \mathbf{D}=0. \end{aligned}\right\} \tag{4.14}$$

A material described by (4.14) in which b and c are constants is referred to as a *Coulomb granular material.*

5. Governing equations

Henceforth, our discussion is limited to a special subclass of cohesionless ($c=\beta_0=0$) Coulomb granular materials in which the density γ is a constant in the non-equilibrium regions. In these regions β and α are, therefore, material constants. This subclass of granular materials is characterized by

$$\left.\begin{aligned} \mathbf{T}&=(-\beta\nu^2+\alpha\nabla\nu\,.\,\nabla\nu+2\alpha\nu\nabla^2\nu)\,\mathbf{1}-2\alpha\nabla\nu\otimes\nabla\nu \\ &\qquad +\lambda(\operatorname{tr}\mathbf{D})\,\mathbf{1}+2\mu\mathbf{D} \quad \text{if} \quad \mathbf{D}\neq 0, \\ s&=-bt \qquad\qquad\qquad\qquad\qquad\quad \text{if} \quad \mathbf{D}=0. \end{aligned}\right\} \tag{5.1}$$

Substituting the dynamic stress relation (5.1) into the balance of linear momentum (2.5), the differential equations

$$\gamma\nu\dot{\mathbf{v}} = -2\beta\nu\nabla\nu + 2\alpha\nu\nabla(\nabla^2\nu) + (\lambda+\mu)\nabla\nabla\cdot\mathbf{v} + \mu\nabla^2\mathbf{v} + \gamma\nu\mathbf{b} \tag{5.2}$$

are obtained. These equations, along with the continuity equation (2.4), constitute the set of governing equations for the non-equilibrium situation.

A dimensional analysis of the differential equations (5.2) shows that, in addition to the usual dimensionless numbers encountered in viscous fluid theory, two more dimensionless parameters are of interest. The dimensionless parameter L, called the *length ratio*, is defined as the ratio of a characteristic geometric length l to the material characteristic length $(\alpha/\beta)^{\frac{1}{2}}$,

$$L = (\beta/\alpha)^{\frac{1}{2}} l. \tag{5.3}$$

The number M,

$$M = \gamma g l/\beta, \tag{5.4}$$

where g is the gravitational constant, is interpreted as the ratio of gravity forces to volume distribution forces.

Possible boundary conditions for granular material theory consist of specifying conditions on the basic fields ν and $\mathbf{v}$ or conditions on the fluxes $\mathbf{T}$ and $\mathbf{h}$, or combinations thereof. The flux boundary conditions are given by

$$\mathbf{T}\mathbf{n} = \mathbf{t}, \tag{5.5}$$

$$\mathbf{h}\cdot\mathbf{n} = H, \tag{5.6}$$

where $\mathbf{t}$ is the customary stress traction and H is the traction associated with the equilibrated stress vector. Since H represents a system of self-equilibrating forces, it does not give rise to a resultant force on the surface and, hence, need not vanish for a free boundary to exist. The equilibrated traction is, however, associated with surface energy per unit area resulting in a type of surface tension effect. If both the equilibrated traction H and the stress traction $\mathbf{t}$ vanish on a boundary, then the boundary is said to be *tension free*.

6. Inclined gravity-flow problem

Consider an infinite slab of granular material of thickness l inclined at an angle ζ to the gravity field and having a tension free upper surface while supported below by a flat plate. A Cartesian co-ordinate system fixed to the upper surface is employed with the x_1 axis oriented down the surface and the x_2 axis normal to the surface.

Although the constitutive relation (5.1) serves to distinguish the material behaviour in the equilibrium situation from that in the non-equilibrium situation, the various regions of equilibrium and non-equilibrium behaviour can only be determined from the solution to the problem. To this end, it is assumed that the various regions in the granular material are characterized by the following assumptions in addition to the constitutive assumption (5.1): For the regions of equilibrium ($D_{ij} = 0$)

(1) $T_{ij} = T_{ij}(x_2)$,

(2) $T_{13} = T_{23} = 0$,

(3) ρ = constant,

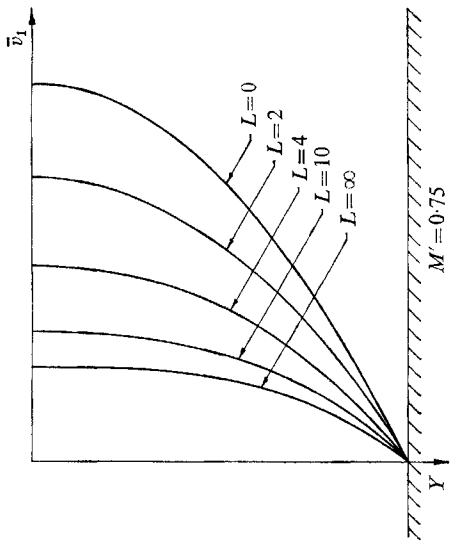

FIGURE 2. Velocity profile for inclined gravity flow.

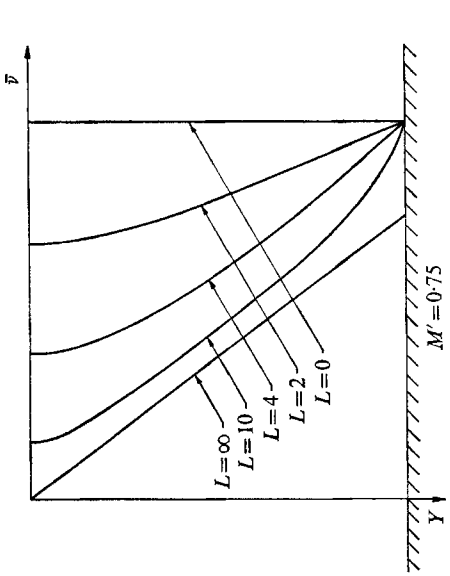

FIGURE 1. Volume distribution profile for inclined gravity flow.

and for the regions of non-equilibrium ($D_{ij} \neq 0$)

(4) steady state, fully-developed flow,

(5) $v_1 = v_1(x_2), \quad v_2 = v_3 = 0,$

(6) $\nu = \nu(x_1, x_2).$

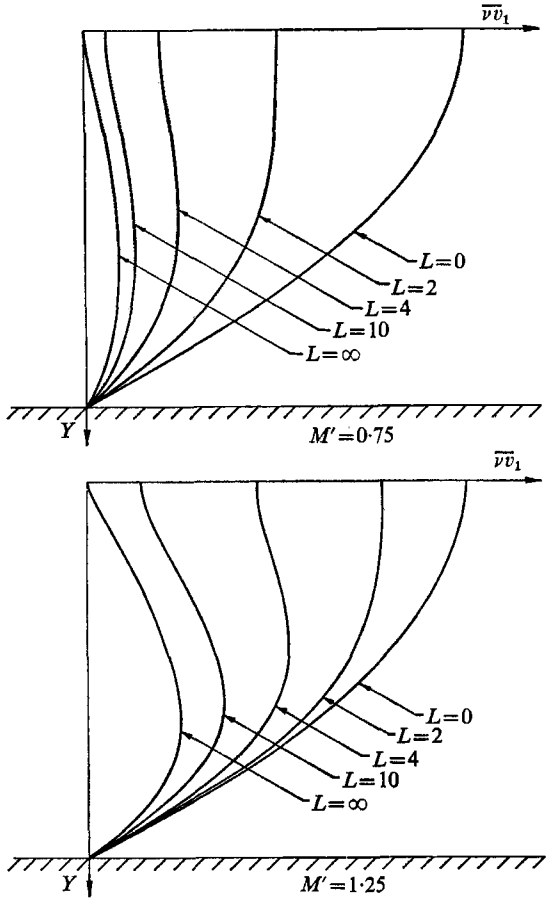

FIGURE 3. Mass flux profile for inclined gravity flow.

From assumptions four and five, the motion is accelerationless and, hence, the balance of linear momentum for both the equilibrium and non-equilibrium regions is given by

$$T_{ij,j} = -\rho b_i. \tag{6.1}$$

Employing assumptions four, five and six in the continuity equation (2.4) restricts the volume distribution in the non-equilibrium regions to $\nu = \nu(x_2)$, from which it follows that the stress in these regions, as well as the equilibrium regions, is a function of the x_2 direction only. Using this fact in (6.1) and recalling that the upper surface $x_2 = 0$ is a free surface, then throughout the medium

$$T_{12}/T_{22} = \cot\zeta. \tag{6.2}$$

Condition (6.2) determines whether the medium is in equilibrium or not. If $\zeta \geqslant \frac{1}{2}\pi - \phi$, where ϕ is the angle of internal friction ($b = \sin\phi$), then the stress state corresponds to a Coulomb stress state and the entire medium is considered to be in equilibrium; otherwise, it is in non-equilibrium. Henceforth, it is assumed that $\zeta < \frac{1}{2}\pi - \phi$.

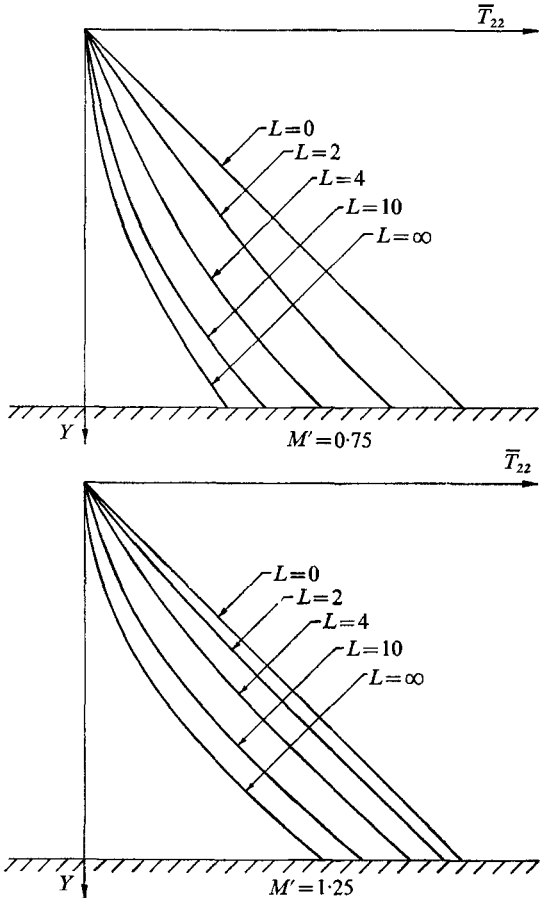

FIGURE 4. Major normal stress profile for inclined gravity flow.

The boundary conditions for this problem are specified at the boundary surface $x_2 = 0$ and along the supporting plate $x_2 = l$. Since the upper surface is tension free, then at $x_2 = 0$

$$T_{12} = T_{22} = 0, \quad h_2 = 0. \tag{6.3}$$

Along the supporting plate the boundary conditions are specified such that at $x_2 = l$,

$$v_1 = v_0, \quad \nu = \nu_0, \tag{6.4}$$

where v_0 is the slip velocity at the plate.

Since the motion is accelerationless and the velocity field divergence free by assumption five above, the governing equations (2.4) and (5.2) become

$$\dot{\nu} = 0, \tag{6.5}$$

$$-2\beta\nu\nu_{,2}+2\alpha\nu\nu_{,222}=-\gamma\nu g\sin\zeta, \tag{6.6}$$

$$\mu v_{1,22}=-\gamma\nu g\cos\zeta. \tag{6.7}$$

Equation (6.5) simply states that the volume distribution at a material point does not change as one follows the motion of the point.

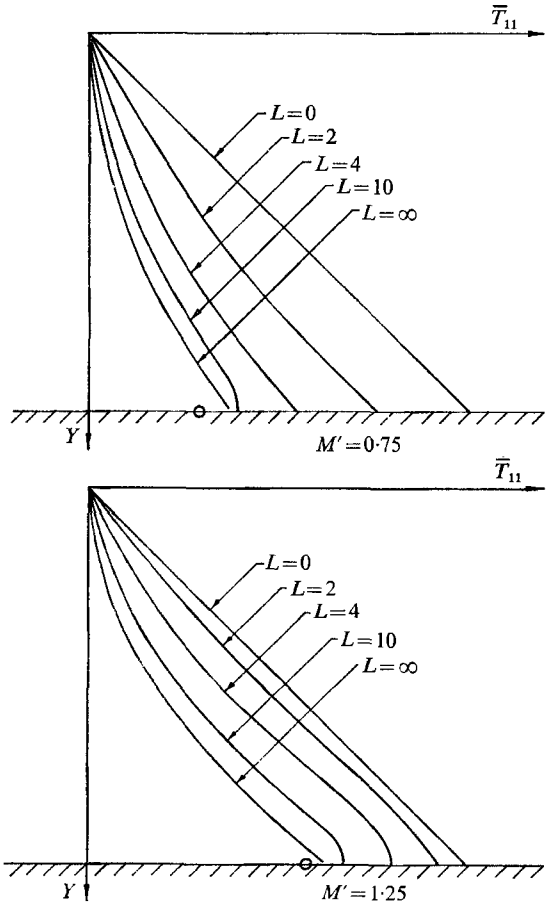

FIGURE 5. Minor normal stress profile for inclined gravity flow.

From (6.6) and (6.7) it is seen that the basic fields uncouple in the sense that (6.6) involves only the volume distribution. Eliminating the trivial solution $\nu = 0$, then (6.6) yields the general solution

$$\nu = A\sinh LY + B\cosh LY + \tfrac{1}{2}MY\sin\zeta + C, \tag{6.8}$$

where A, B and C are arbitrary constants of integration, L and M are the non-dimensional quantities defined by (5.3) and (5.4) and Y is a dimensionless co-ordinate defined by

$$Y = x_2/l. \tag{6.9}$$

Employing (6.8) in (6.7), the velocity field is then easily obtained,

$$v_1 = -\frac{\gamma g l^2\cos\zeta}{\mu}\left[\frac{A}{L^2}\sinh LY + \frac{B}{L^2}\cosh LY + \frac{M}{12}Y^3\sin\zeta + \tfrac{1}{2}CY^2 + DY + E\right], \tag{6.10}$$

where D and E are additional integration constants. Evaluating the five constants of integration from the boundary conditions (6.3) and (6.4) and introducing the non-dimensional parameter

$$M' = M(\sin\zeta)/2\nu_0 = \gamma g l(\sin\zeta)/2\beta\nu_0, \tag{6.11}$$

then (6.8) becomes

$$\frac{\nu}{\nu_0} = -M'\frac{\sinh LY}{L} + \left(1 - M' + M'\frac{\sinh L}{L}\right)\left(\frac{1+\cosh LY}{1+\cosh L}\right) + M'Y \tag{6.12}$$

and (6.10) can be expressed as

$$\begin{aligned} v_1 - v_0 = \frac{\gamma\nu_0 g l^2\cos\zeta}{2\mu}\Bigg[& -2\frac{M'}{L^3}(\sinh L - \sinh LY) \\ & + \left(1 - M' + M'\frac{\sinh L}{L}\right)\left(\frac{1-Y^2}{1+\cosh L}\right) + \frac{2}{L^2}\left(1 - M' + M'\frac{\sinh L}{L}\right) \\ & \times \left(\frac{\cosh L - \cosh LY}{1+\cosh L}\right) + \frac{M'}{3}(1-Y^3) + \frac{2M'}{L^2}(1-Y)\Bigg]. \end{aligned} \tag{6.13}$$

The expressions (6.12) and (6.13) for the volume distribution and velocity show that the solution depends strongly on the dimensionless length ratio L and the dimensionless constraining number M'. The constraining number represents the effect of the external constraints since it is defined in terms of the gravity field and boundary conditions.

We consider now the limiting cases in which the length ratio L approaches zero and infinity, respectively. These two limiting cases form the bounding solutions and, hence, delimit the influence of volume distribution on the material behaviour. For the limiting case described by $L = 0$, it can be shown that (6.12) and (6.13) become

$$\nu/\nu_0 = 1, \tag{6.14}$$

$$v_1 - v_0 = (\gamma\nu_0 g l^2/2\mu)(\cos\zeta)(1 - Y^2), \tag{6.15}$$

and the normal stresses determined from the constitutive relation (5.1) are given by

$$T_{11} = T_{22} = -\gamma\nu_0 g l(\sin\zeta)\, Y. \tag{6.16}$$

These representations show that the granular material solution reduces to that of an incompressible Navier–Stokes fluid. This solution is independent of the parameter M' indicating that the externally imposed boundary conditions and gravity field do not distort the shape of the stress and velocity profiles from their classical linear and parabolic shapes, respectively.

The upper limiting case represented by L tending to infinity is characterized by

$$\frac{\nu}{\nu_0} = \begin{cases} M'Y & (0 \leqslant Y < 1), \\ 1 & (Y = 1), \end{cases} \tag{6.17}$$

$$v_1 - v_0 = \frac{\gamma\nu_0 g l^2\cos\zeta}{2\mu}\tfrac{1}{3}M'(1 - Y^3), \tag{6.18}$$

$$T_{22} = -\gamma\nu_0 g l(\sin\zeta)\, M'\tfrac{1}{2}Y^2, \tag{6.19}$$

$$T_{11} = \begin{cases} -\gamma\nu_0 g l(\sin\zeta)\tfrac{1}{2}M'Y^2 & (0 \leqslant Y < 1), \\ -\gamma\nu_0 g l(\sin\zeta)(2 - \tfrac{1}{2}M' - (1/M')) & (Y = 1). \end{cases} \tag{6.20}$$

Just as the lower limiting solution represents the least effect of volume distribution on the solution, the limiting case $L \to \infty$ represents the greatest effect. As the length ratio increases, the influence of volume distribution becomes more pronounced. The discontinuity in the solution at the supporting plate ($Y = 1$) is a boundary effect. For large values of length ratio L, the volume distribution and minor normal stress vary strongly in a small region near the boundary. If M' equals unity, however, the discontinuities at the boundary vanish. This strong dependence on M' demonstrates the important effect of the external constraints.

Profiles for the volume distribution, dimensionless velocity, and dimensionless stress defined by

$$\bar{\nu} = \frac{\nu}{\nu_0}, \quad \bar{v}_1 = \frac{2\mu(v_1 - v_0)}{\gamma \nu_0 g l^2 \cos\zeta}, \quad \bar{\mathbf{T}} = \frac{-\mathbf{T}}{\gamma \nu_0 g l \sin\zeta} \tag{6.21}$$

and also for the dimensionless mass flux $\bar{\nu}\bar{v}_1$ are shown in figures 1 to 5. These plots are presented for specified values of M' over the entire range of length ratio L and form two sets of curves; one set with M' less than unity and the other with M' greater than unity. Figure 1 illustrates the strong dependence of volume distribution on M'. For $M' < 1$, the volume distribution increases monotonically with depth, whereas, for $M' > 1$, the volume distribution attains a local maximum. The boundary effect for large length ratios is particularly evident in this figure. Figure 3 shows the interesting result that the maximum mass flux in the flow does not necessarily occur at the upper surface. There is no parallel to this type of behaviour in incompressible fluid theory. Figures 4 and 5 show the normal stress distributions to be non-linear for non-zero length ratios. Moreover, the magnitudes of the major and minor stresses are unequal and also less than that predicted by hydrostatic pressure theory.

7. Vertical channel-flow problem

In this section, the problem of flow of a granular material between two infinite parallel flat plates aligned with the gravity field is considered. The plates are spaced a distance $2l$ apart and a Cartesian co-ordinate system centred between the plates is employed. The x_1 axis is oriented normal to the plates and the x_2 axis is along the direction of flow.

As in the previous problem, the assumptions concerning flow in regions of equilibrium and non-equlibrium are presented as follows: For the regions of equilibrium,

(1) $T_{ij} = T_{ij}(x_1)$,

(2) $T_{13} = T_{23} = 0, \quad T_{12}(x_1) = -T_{12}(-x_1)$,

(3) ρ = constant,

and for the regions of non-equilibrium,

(4) steady state, fully-developed flow,

(5) $v_2 = v_2(x_1) = v_2(-x_1), \quad v_1 = v_3 = 0$,

(6) $\nu = \nu(x_1, x_2) = \nu(-x_1, x_2)$.

From the above assumptions it follows that the motion is accelerationless and that the stresses throughout the medium are only a function of the x_1 direction. Hence, the balance of linear momentum yields the component equations

$$T_{11,1} = 0, \tag{7.1}$$

$$T_{21,1} = -\gamma\nu g. \tag{7.2}$$

Integrating (7.1) gives

$$T_{11} = -T_0, \tag{7.3}$$

where T_0 is a constant. Since T_{12} must be an odd function of x_1, then

$$T_{12}(0) = 0. \tag{7.4}$$

For non-zero T_0, the stress state described by the relations (7.3) and (7.4) must be a Coulomb stress state and, consequently, the material in the centre of the channel must be in equilibrium. This equilibrium condition implies the existence of a uniform velocity, or plug flow, in the centre region. The interface distance between the plug region and shearing region is denoted by $x_1 = \pm a$ and is introduced as an unknown to be determined by the solution to the problem.

The boundary conditions are specified along the constraining plates. It is assumed that at $x_1 = \pm l$

$$v_2 = v_0, \quad \nu = \nu_0. \tag{7.5}$$

The differential equations for the non-equilibrium region are given by

$$\nu_{,111} - (\beta/\alpha)\nu_{,1} = 0, \tag{7.6}$$

$$\mu v_{2,11} = -\gamma\nu g, \tag{7.7}$$

which yield the solutions

$$\nu = A\cosh LX + B\sinh LX + C \tag{7.8}$$

and

$$v_2 = -\frac{\gamma g l^2}{\mu}\left[\frac{A}{L^2}\cosh LX + \frac{B}{L^2}\sinh LX + \tfrac{1}{2}CX^2 + DX + E\right], \tag{7.9}$$

where A, B, C, D, E are integration constants, L is the non-dimensional length ratio and X is a dimensionless co-ordinate defined by

$$X = x_1/l. \tag{7.10}$$

Employing assumptions five and six which restrict the volume distribution and velocity field to be even functions, then one must require

$$B = D = 0. \tag{7.11}$$

Noting that the volume distribution must satisfy the stress condition

$$T_{11}(\pm l) = -T_0, \tag{7.12}$$

then the remaining integration constants can be determined from (7.12) and the boundary conditions (7.5). Introducing the dimensionless parameter

$$M'' = MT_0/\gamma\nu_0^2 gl = T_0/\beta\nu_0^2, \tag{7.13}$$

then (7.8) and (7.9) can be expressed as

$$\frac{\nu}{\nu_0} = 1 - \left(\frac{\cosh L \pm (1 + M''\sinh^2 L)^{\frac{1}{2}}}{\sinh^2 L}\right)(\cosh L - \cosh LX), \tag{7.14}$$

$$v_2 - v_0 = \frac{\gamma\nu_0 g l^2}{2\mu}\left[\frac{2}{L^2}\left(\frac{\cosh L \pm (1 + M''\sinh^2 L)^{\frac{1}{2}}}{\sinh^2 L}\right)(\cosh L - \cosh LX) - \left(\frac{1 \pm \cosh L(1 + M''\sinh^2 L)^{\frac{1}{2}}}{\sinh^2 L}\right)(1 - X^2)\right]. \tag{7.15}$$

The parameter M'' appearing in the expressions (7.14) and (7.15) is a constraining number analogous to M' of the previous problem. Along with the length ratio L, it characterizes the flow. The number M'' represents the effect of the pressure T_0 from the confining plates. Unlike M', it does not explicitly involve the gravity field or the geometric length.

From (7.14) and (7.15) it is seen that the problem has two solutions depending on the sign of the square root. However, upon determining the stresses from the

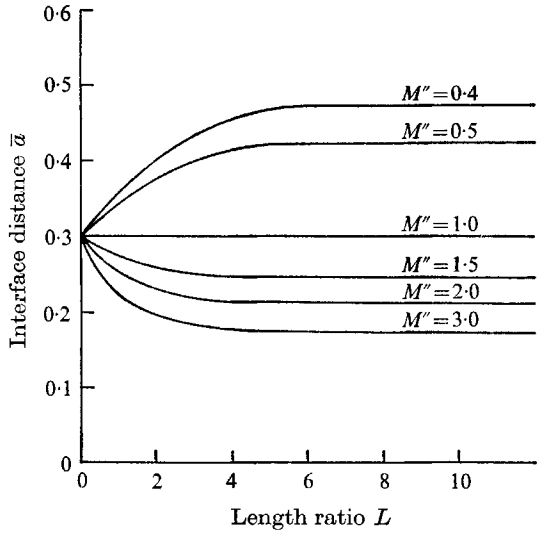

FIGURE 6. Interface distance for vertical channel flow problem ($S = 0·3$).

constitutive relation (5.1), it is noted that the solution involving the positive square root must yield positive normal stresses T_{22}. Since cohesionless granular materials cannot generally support tensile stresses, this constraint is physically unrealistic. The solution with the positive square root is consequently disregarded. The solution for the problem is based on the negative square root.

Recalling that the central region of the channel is in equilibrium characterized by plug flow, then the above solution is only valid in the regions near the channel walls. To determine the interface distance $x_1 = \pm a$ between the plug and shearing regions, note that the Coulomb condition

$$T_{12} = -T_0 \tan\phi \tag{7.16}$$

must be satisfied at the interface. Requiring the shear stress to be continuous across the interface, then the value of the shear stress given by (7.16) must correspond with the value computed from (7.15). Denoting the dimensionless interface distance and dimensionless Coulomb shear stress by

$$\bar{a} = a/l, \quad S = T_0 \tan\phi/\gamma v_0 g l, \tag{7.17}$$

then one obtains the condition

$$\left(\frac{\cosh L - (1 + M'' \sinh^2 L)^{\frac{1}{2}}}{L \sinh^2 L}\right) \sinh L\bar{a} - \left(\frac{1 - \cosh L(1 + M'' \sinh^2 L)^{\frac{1}{2}}}{\sinh^2 L}\right) \bar{a} = S, \tag{7.18}$$

which serves to determine the interface distance in terms of the parameters L, M'' and S. Using the value of $\bar{a}$, the new dimensionless variable

$$\bar{X} = \frac{X-\bar{a}}{1-\bar{a}} \quad (0 \leqslant \bar{X} \leqslant 1) \tag{7.19}$$

can then be introduced into the expressions (7.14) and (7.15) and, in this way, restrict these expressions to the shearing region defined by $\bar{a} \leqslant X \leqslant 1$. A plot of dimensionless interface distance $\bar{a}$ *versus* length ratio L is shown in figure 6

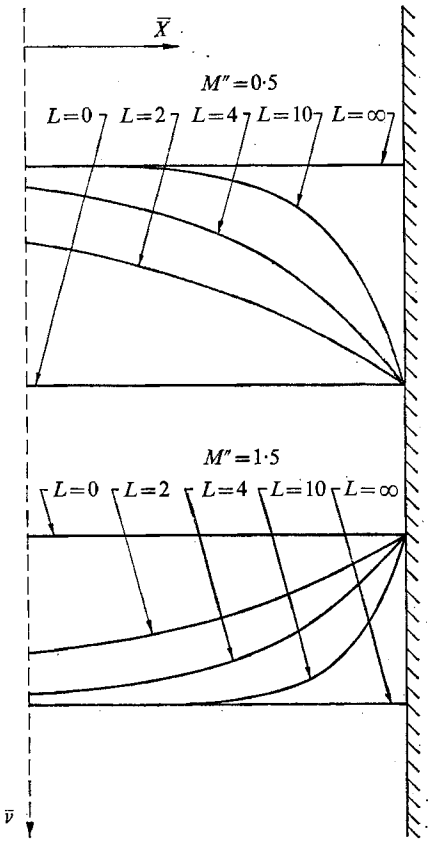

FIGURE 7. Volume distribution profile for vertical channel flow.

for selected values of M'' and the parameter S. For $M'' > 1$, the interface distance (or, equivalently, the width of the plug region) decreases as L increases; for $M'' < 1$, the converse situation results. $M'' = 1$ represents a critical situation in which the interface distance is a constant for all values of L.

The limiting cases for the channel-flow problem will now be discussed. For $L = 0$, the solution is given by

$$\nu/\nu_0 = 1, \tag{7.20}$$

$$v_2 - v_0 = (\gamma\nu_0 g l^2/2\mu)(1-X^2), \tag{7.21}$$

$$T_{11} = T_{22} = -T_0. \tag{7.22}$$

As in the inclined gravity-flow problem, the lower limiting case corresponds to the solution for an incompressible fluid. However, in this problem, the granular

material behaves more like a Bingham fluid in that a region of plug flow exists. Note that the pressure does not increase with depth, but is a constant throughout the shearing region.

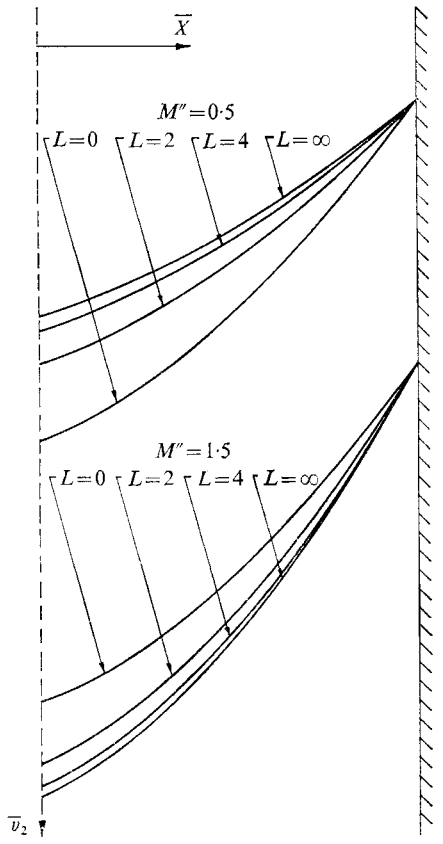

FIGURE 8. Velocity profile for vertical channel flow.

For the upper limiting case, the following expressions are obtained:

$$\frac{\nu}{\nu_0} = \begin{cases} \sqrt{M''} & (0 \leqslant X < 1), \\ 1 & (X = 1), \end{cases} \tag{7.23}$$

$$v_2 - v_0 = (\gamma \nu_0 g l^2/2\mu)\,(\sqrt{M''})\,(1 - X^2), \tag{7.24}$$

$$T_{11} = -T_0, \tag{7.25}$$

$$T_{22} = \begin{cases} -T_0 & (0 \leqslant X < 1), \\ -(T_0/M'')\,(4(\sqrt{M''}) - M'' - 2) & (X = 1). \end{cases} \tag{7.26}$$

Once again, the discontinuities at the walls are indicative of a boundary effect. If $M'' = 1$, the discontinuities at the boundary vanish. The solution then reduces to that of the lower limiting case, and since the two limiting solutions are the bounding solutions for the problem, it follows that every solution must be identical. In this critical condition, the granular material behaves as an incompressible fluid irrespective of the length ratio L.

Dimensionless forms of the volume distribution and velocity,

$$\bar{\nu} = \nu/\nu_0, \quad \bar{v}_2 = 2\mu(v_2 - v_0)/\gamma\nu_0 g l^2, \tag{7.27}$$

as well as the dimensionless mass flux $\overline{\nu v}_2$, are shown in figures 7, 8, and 9, respectively, for specified values of M'' and for the complete range of L. The curves are presented for M'' greater and less than unity and are plotted against the

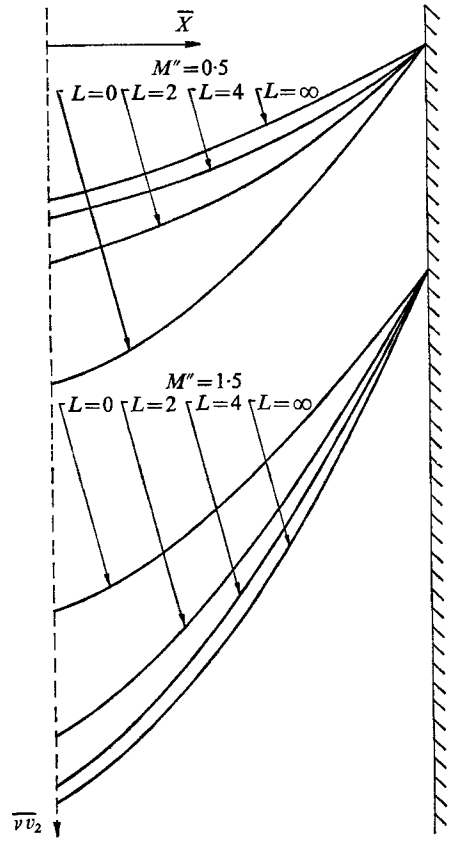

FIGURE 9. Mass flux profile for vertical channel flow.

non-dimensional co-ordinate $\bar{X}$ defined by (7.19) so that only the region outside the plug is represented. The figures show that the magnitude of M'' relative to unity strongly influences the solution to the problem. As illustrated in figure 7, the volume distribution increases monotonically from the plug to the wall for $M'' < 1$ and decreases monotonically for $M'' > 1$. Also the velocity and mass flux profiles 'fan out' in a direction that is dependent on M''. If $M'' < 1$, the profiles decrease with L whereas, if $M'' > 1$, the profiles increase with L.

To conclude this section, consider the problem of optimizing the flow rate through the channel. For a given granular material and a given channel width (or, equivalently, for a given length ratio L), the flow rate is governed by the constraining number M''. Since the mass flux increases with M'' and the maximum

flux in the channel occurs in the plug region, one would expect the optimum flow rate to be achieved by maximizing M''. However, figure 6 shows that the width of the plug region decreases as M'' increases. Consequently, the optimum flow rate through the channel may be achieved at some intermediate value of M''.

8. Concluding remarks

The results presented here for inclined gravity flow and vertical channel flow of a granular material demonstrate the importance in the present theory of the two dimensionless numbers, the length ratio L and a constraining number M' or M''. The length ratio represents the effect of volume distribution on the dynamical behaviour whereas the constraining number represents the effect of external constraints such as the gravity field and boundary conditions. For small values of length ratio, it is shown that the material response is essentially that of an incompressible viscous fluid. From this result one might conjecture that the length ratio is associated with the material grain size since granular materials composed of 'small' granules are known to behave in a fluid-like fashion. Materials with large grains exhibit behaviour quite distinct from fluid behaviour.

Since a collection of granules forms a granular body only by virtue of a constraining force field, like a body force field, or by virtue of being confined in a container, it is apparent that the constraining numbers M' and M'' are very significant parameters in the theory. Indeed, for the two problems considered, if there is no gravity field ($g = 0$) or no constraining plates ($T_0 = 0$), then M' and M'' are zero and it follows that the normal stresses must also be zero. Conversely, requiring the normal stresses to be non-zero implies that M' and M'' must be non-zero. Although, by definition, M' and M'' are only restricted to be positive, the range of values for the constraining numbers must depend on the boundary conditions and body force field which admit physically realistic values for the stresses. The range of values for M' and M'' used in this study were determined from the normal stress representations (6.20) and (7.26). Requiring the minor normal stress to be compressive for the entire range of length ratios considered, including the upper limiting case, then the following restrictions were obtained:

$$0{\cdot}5 \leqslant M' \leqslant 2+\sqrt{2}, \tag{8.1}$$

$$0{\cdot}5 \leqslant \sqrt{M''} \leqslant 2+\sqrt{2}. \tag{8.2}$$

These inequalities show that the requirement that all normal stresses be compressive severely limits the range of the constraining numbers. From these restrictions and the definitions (6.11) and (7.13) for M' and M'', respectively, it follows that the ratio of boundary volume distribution ν_0 to the confining force, ν_0^2/T_0 and $\nu_0/\gamma g l$, vary little for these problems.

Some experimental evidence for the results obtained in this investigation exists. Among the early experimental work in the flow of granular materials is that of Howard (1939). The solid concentration, velocity, and mass flux profiles determined by Howard for the flow of sand in a 4 in. pipe are in qualitative agreement with the results for inclined flow if $M' < 1$. Of interest is the local maximum obtained for the mass flux profile. Commenting on the investigation

of Howard, Danel (1939) notes that "if the concentration distribution is fairly uniform...the conditions are nearly those of an homogeneous fluid". This statement is consistent with the predicted behaviour for small length ratios. Later work by Durand (1953) and Newitt, Richardson & Shook (1962) with fine sands confirm the findings of Howard. In addition, Newitt, Richardson & Shook show that coarse materials such as coarse sands and gravel exhibit solid concentration profiles like those for the case when $M' > 1$.

For two-phase gas–solid flow of 50 μ glass particles, Soo *et al.* (1964) observed that "the nature of the concentration, mass flow, and velocity distributions of solid particles is such that the concentration increases toward the wall of the pipe, mass flow decreases toward the wall, and velocity is less than or equal to that of the stream at the core". These observations are in agreement with the results for channel flow if $M'' < 1$. Similar experimental data was obtained by Van Zoonen (1962) who employed 20–100 μ particles. Experimental evidence for a decrease in solid concentration toward the wall of a square duct is given by Peskin & Dwyer (1965). This gives qualitative support to the analytical results for $M'' > 1$.

We thank a referee for criticism that led to an improvement in this paper.

This work was supported, in part, by the U.S. Army Research Office in Durham under Grant DA-ARO-D-31-124-G599 with Tulane University.

REFERENCES

Danel, P. F. 1939 *Trans. ASCE* **104**, 1373.

Deresiewicz, H. 1958 *Adv. Appl. Mech.* **5**, 233.

Drucker, D. C., Gibson, R. E. & Henkel, D. J. 1957 *Trans. ASCE* **122**, 338–346.

Drucker, D. C. & Prager, W. 1952 *Quart. Appl. Math.* **10**, 157.

Durand, R. 1953 *Proc. Minnesota Hydraulic Conv.*

Goodman, M. A. 1970 Ph.D. Thesis, Tulane University.

Howard, G. W. 1939 *Trans. ASCE* **104**, 1335–1348.

Jenike, A. W. & Shield, R. T. 1959 *J. Appl. Mech.* **26**, 599.

Leva, M. 1959 *Fluidization.* McGraw-Hill.

Love, A. E. H. 1926 *On the Mathematical Theory of Elasticity.* Dover.

Murray, J. D. 1965 *J. Fluid Mech.* **21**, 465.

Newitt, D. M., Richardson, J. F. & Shook, C. A. 1962 *Proc. Symposium on Interaction Between Fluids and Particles*, Inst. Chem. Engrs.

Peskin, R. L. & Dwyer, H. A. 1965 *ASME Paper* 65-WA/FE-24.

Reynolds, O. 1885 *Phil. Mag.* **20**, 469–481.

Rowe, P. W. 962 *Proc. Roy. Soc.* A **269**, 500.

Shield, R. T. 1955 *J. Mech. Phys. Solids*, **4**, 10.

Soo, S. L. 1967 *Fluid Dynamics of Multiphase Systems.* Blaisdell.

Soo, S. L., Trezek, G. J., Dimick, R. C. & Hohnstreiter, G. F. 1964 *Ind. Engng Chem. Fund.* **3**, 98.

Spencer, A. J. M. 1964 *J. Mech. Phys. Solids*, **12**, 337.

Van Zoonen, D. 1962 *Proc. Symposium on Interaction Between Fluids and Particles*, Inst. Chem. Engrs.

Winterkorn, H. F. 1966 *Princeton Soil Eng. Res. Series*, no. 7, Contract no. AF19(628)-2414.

Zenz, F. A. & Othmer, D. F. 1960 *Fluidization and Fluid-Particle Systems.* Reinhold.